

# Plasmonic Nearfield Scanning Probe with High Transmission

Yuan Wang,<sup>†</sup> Werayut Srituravanich,<sup>†</sup> Cheng Sun,<sup>†</sup> and Xiang Zhang<sup>\*,†,‡</sup>

National Science Foundation (NSF) Nanoscale Science and Engineering Center (NSEC), 5130 Etcheverry Hall, University of California, Berkeley, California 94720-1740, and Materials Sciences Division, Lawrence Berkeley National Laboratory, 1 Cyclotron Road, Berkeley, California 94720

Received August 5, 2008

## ABSTRACT

Nearfield scanning optical microscopy (NSOM) offers a practical means of optical imaging, optical sensing, and nanolithography at a resolution below the diffraction limit of the light. However, its applications are limited due to the strong attenuation of the light transmitted through the subwavelength aperture. To solve this problem, we report the development of plasmonic nearfield scanning optical microscope with an efficient nearfield focusing. By exciting surface plasmons, plasmonic NSOM probes are capable of confining light into a 100 nm spot. We show by nearfield lithography experiments that the intensity at the near field is at least one order stronger than the intensity obtained from the conventional NSOM probes under the same illumination condition. Such a high efficiency can enable plasmonic NSOM as a practical tool for nearfield lithography, data storage, cellular visualization, and many other applications requiring efficient transmission with high resolution.

Nearfield scanning optical microscopy and its variations combine the scanning probe technology with optical microscopy and have been applied intensively in the study of biology,<sup>1,2</sup> material science,<sup>3,4</sup> and data storage.<sup>5</sup> NSOM offers a practical means of optical imaging and sensing, as well as nanolithography, all with resolution well beyond the diffraction limit of the light. However, its applications are somewhat limited by the strong attenuation of the light transmitted through the subwavelength aperture. For example, the optical transmission of a NSOM probe with a sub-100 nm opening is typically on the order of  $10^{-5}$  to  $10^{-7}$ ,<sup>6</sup> resulting in a long measurement time for imaging purposes or a long exposure time for lithography applications. Clearly, a light source with subwavelength size and high intensity will be very useful for applications including nanolithography, high-density data storage, nanospectroscopy, biosensing, molecular trapping, and so forth. Several methods have been proposed to generate sub-diffraction-limited intense light spot. For examples, H-shaped, C-shaped, and bowtie-shaped apertures can provide strong optical throughput through the subwavelength apertures.<sup>7-11</sup> However, advances in this scheme are still limited to planar structures, which greatly restrict practical applications in NSOM techniques. While NSOM relies on a point contact during the scanning process which can ensure the proper feedback for maintaining the probe-sample separation, planar structures with given dimen-

sions will restrict the stability of scanning and may lead to damages on sample surfaces. We integrate a nanoaperture surrounded by a circular through grating, namely, a *plasmonic lens*,<sup>12</sup> on the metal coating of a conic NSOM probe (similar to the structures studied recently on the farfield transmission<sup>13</sup>). The conic plasmonic lens can focus light energy into a sub-diffraction-limited intense spot which enables probing the sample in the near field with high resolution and high efficiency.

Surface plasmon polaritons (SPPs) are collective electron oscillations propagating along a metal dielectric interface that can be excited by light using nanostructures.<sup>14</sup> The wavelength of SPP waves can be estimated by

$$\lambda_{\text{sp}} = \lambda_0 \sqrt{(\epsilon_d + \epsilon_m) / (\epsilon_d \epsilon_m)}$$

where  $\lambda_0$  is the illumination light wavelength in free space, and  $\epsilon_m$  and  $\epsilon_d$  are the dielectric constants of metal and surrounding dielectric, respectively. When  $\epsilon_m$  is approaching  $-\epsilon_d$  at certain wavelengths, the  $\lambda_{\text{sp}}$  becomes much smaller than  $\lambda_0$ . This unique dispersive behavior of SPPs allows for the manipulation of light at subwavelength scale compared to the excitation light.<sup>15</sup> In addition, the electromagnetic field of SPPs can be significantly amplified due to the resonance effect.<sup>16</sup> Owing to the aforementioned special properties, SPPs have opened up new applications such as subwavelength lithography,<sup>17-20</sup> optical data storage,<sup>21</sup> and molecular sensing.<sup>22,23</sup> The SPP mediated extraordinary transmission through a periodic array of subwavelength holes also stimulated extensive studies.<sup>24-28</sup>

Focusing SPP energy into an ultrasmall spot is of special

\* e-mail: xiang@berkeley.edu.

<sup>†</sup> NSEC.

<sup>‡</sup> Lawrence Berkeley National Laboratory.

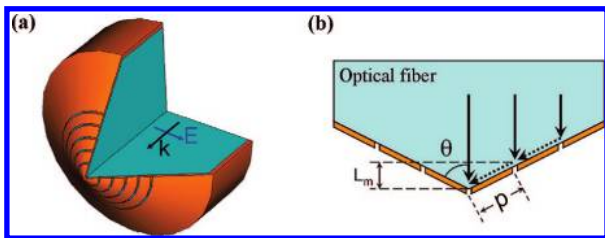


**Figure 1.** (a) Schematic drawing of the conic plasmonic lens. (b) Illustration of interference between the SPP waves generated by the inner rings and those transmitted SPP waves from the outer rings. Solid and dashed arrows represent incident light and SPPs, respectively.

interest due to its potential applications in subwavelength lithography, imaging, and sensing. Various metal structures, including bull's eye structures,<sup>29,30</sup> curved nanometric hole arrays,<sup>31</sup> and single or multiple circular rings,<sup>12,32</sup> have been investigated to excite and focus SPPs. While most of the efforts were concentrated on designing better structures to focus SPPs on a planar metal surface,<sup>33–36</sup> special applications on nonplanar samples request new plasmonic focusing devices design with three-dimensional geometries, such as conic or pyramidal SPP lenses. In this paper, we present a design of conic plasmonic lens integrated on the tapered tip of a NSOM probe to enhance the transmission and generate an intense light spot with subwavelength dimensions. Moreover, with this plasmonic lens, only the apex of the conic structure interacts with the sample surface during the approaching and scanning process of plasmonic NSOM, which thereby increases the NSOM sensitivity.

The new conic plasmonic lens consists of a subwavelength aperture at the apex of the cone surrounded by through concentric rings in a thin Al film deposited on a tapered fiber tip, as shown in Figure 1. The lens geometry enforces all the SPPs generated by the rings to travel toward the apex at the center due to the geometry. To obtain the best transmission efficiency through the aperture, the spacing between the rings and the tapering angle of the NSOM tip should be designed to provide the constructive interference conditions of lights and SPPs at the center aperture. For simplicity, we take the dielectric constant on either side of the plasmonic lens to be the same, which can be achieved by using index matching oil in experiments. Considering the constructive interference between light propagating directly from the media with a phase delay  $\Delta\phi_m = 2\pi \cdot L_m / \lambda_m$  and SPPs propagating along the metal surface with a phase delay  $\Delta\phi_{sp} = 2\pi \cdot p / \lambda_{sp}$ , eq 1 should be satisfied, where  $\lambda_m$  is wavelength in the media,  $L_m$  is the propagating distance when the light meets the SPP excited by the light from the same wavefront,  $p$  is the spacing between the rings as mentioned before, and  $\lambda_{sp}$  is the SPP wavelength on the metal surface.

$$|\Delta\phi_{sp} - \Delta\phi_m| = 2n\pi \quad (1)$$

For a conic structure with cone angle  $\theta$ , we have

$$L_m = p \cdot \cos \theta \quad (2)$$

Considering  $\lambda_{sp} < \lambda_m$ ,<sup>14</sup> we get the smallest positive value of  $p$  when  $n = 1$  (e.g., the condition of constructive interference):

$$\frac{1}{p} = \frac{1}{\lambda_{sp}} - \frac{\cos \theta}{\lambda_m} \quad (3)$$

We have applied nearfield lithography to demonstrate the enhanced nearfield transmission of the proposed conic

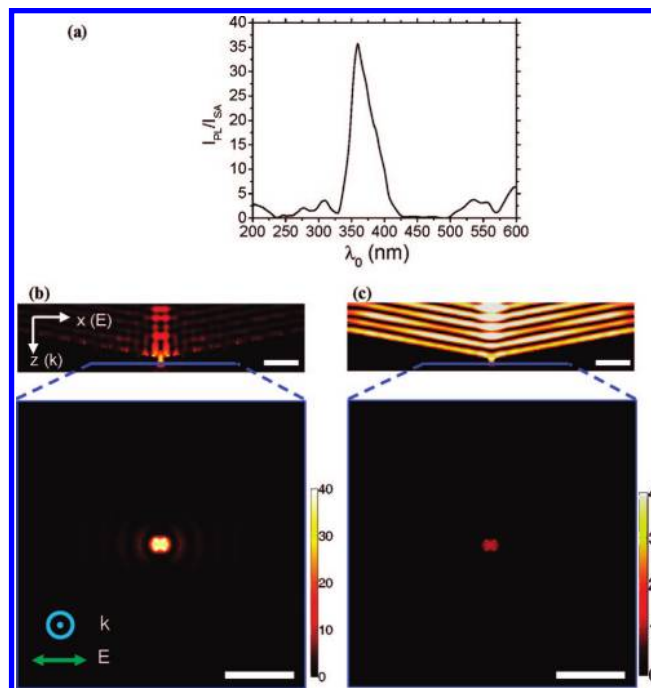


**Figure 2.** (a) Enhancement factor of the light intensity at the focal point through a plasmonic lens ( $I_{PL}$ ) compared to that through a single aperture ( $I_{SA}$ ) versus the illumination wavelength. The aperture diameter, ring periodicity, ring width, and aluminum layer thickness are 100, 300, 50, and 100, respectively, and the cone angle is  $75^\circ$ . (b) Simulated intensity of the near field of the plasmonic lens under the linearly polarized plane wave illumination with the wavelength of 365 nm. (c) Simulated intensity of the near field of a single aperture under the same illumination as in (b). The scale bars in (b) and (c) are 500 nm.

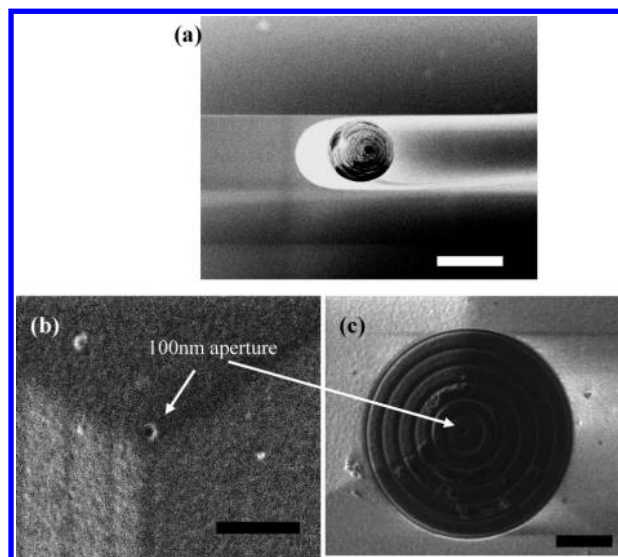


**Figure 3.** (a) NSOM probe consists of nanostructured plasmonic lens being fabricated on the end of a optical fiber. 100 nm aperture on the NSOM tip (b) before and (c) after the fabrication of the plasmonic lens. Scale bar in (a) is 100  $\mu\text{m}$ ; those in (b) and (c) are 1  $\mu\text{m}$ .

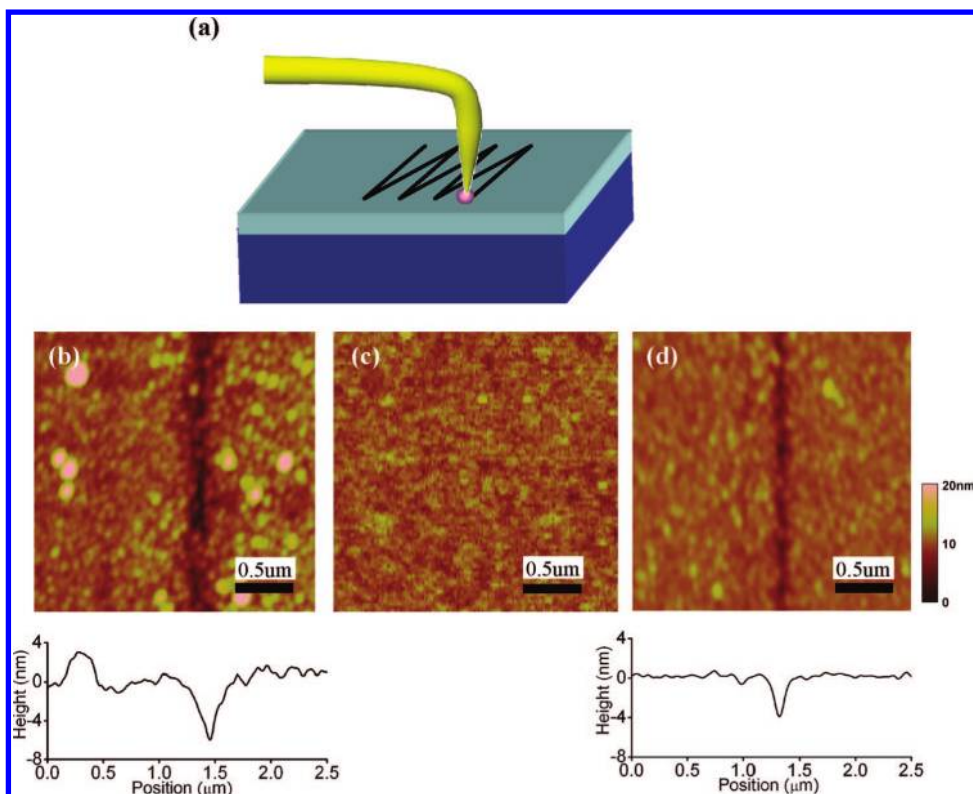


**Figure 4.** (a) Schematic illustration of nearfield scanning lithography. (b) AFM image of the photoresist after nearfield scanning exposure of 0.008 mW using the plasmonic lens. (c) Same as (b) but with single aperture NSOM probe (without the plasmonic lens). (d) Control experiment by single aperture NSOM probe with an input laser power of 0.08 mW. The fwhm and depth of patterned lines in (b) and (d) are 124, 6.8, 97, and 4.2 nm, respectively.

plasmonic lens, so the working wavelength was selected at 365 nm for the convenience of the photolithography process. Aluminum was chosen for its good coating quality on NSOM probes.  $\lambda_m$  and  $\lambda_{sp}$  thus can be determined by the refractive index of the fiber ( $n = 1.52$ ) and the aluminum permittivity ( $\epsilon_m = -19.4 + 3.6i$ ).<sup>37</sup> Therefore, the period of the rings solely relies on the cone angle  $\theta$ . Recently, 2-D simulations have shown that total light transmission of a tip can be enhanced by a factor of 10 by the corrugation of metal coating.<sup>38</sup> In our work, we employed 3-D numerical simulations to obtain a practical combination of the optimized parameters, namely, aperture diameter, ring width, and metal layer thickness, for both field confinement and enhancement factor at the apex. The 3-D simulations were carried out using commercial FDTD software (CST Microwave Studio) under a linearly polarized plane wave illumination. The simulated plasmonic lens is composed of a nanoaperture surrounded by 6 through rings in aluminum film. The cone angle was set to 75° in our model by the convenience of our fabrication process, which will be addressed later. The best ring periodicity can be obtained as 300 nm from eq 3. The optimized sizes for aperture diameter, ring periodicity, ring width, and aluminum layer thickness are 100, 50, and 80 nm, respectively. Figure 2a shows the wavelength dependence of the intensity enhancement factor of the plasmonic lens normalized to the intensity without rings. The peak enhancement factor of about 36 times is observed at 365 nm which is exactly our designed wavelength. To make a side-by-side comparison, Figure 2b and 2c show the profile

of E-field amplitude of a single aperture with and without the plasmonic lens (notice the difference in the color bars). The cross-sectional view of the intensity profile at the plane near the aperture shows a very good field confinement with spot size of  $\sim 100$  nm along the  $x$ -direction and  $\sim 85$  nm in the  $y$ -direction. This asymmetry is due to the horizontal polarization of the incident light.

The plasmonic NSOM tip was modified from an optical fiber bent 90° by a CO<sub>2</sub> laser beam (Figure 3a). First, the NSOM tip was tapered using focused ion beam milling (FIB, FEI Strata 201 XP) to generate a tip apex with a 75° taper angle. Subsequently, the tip apex was coated with 100 nm thick aluminum using e-beam deposition (Edwards EB3 E-beam Evaporator). We note that the coating is 20 nm thicker than the designed thickness. Simulation shows that local field enhancement for this thickness is still 90% of the optimal condition. In the first step of plasmonic lens fabrication, only a 100 nm aperture was milled by FIB at the tip apex (Figure 3b). Control experiment data were collected with these single aperture tips, as is discussed below. After that, the same tips were further milled by FIB to fabricate a plasmonic lens around the aperture (Figure 3c). Because this actual plasmonic-NSOM probe tapered by FIB has a three-sided pyramid shape instead of a conical shape in simulation, the cone angle was chosen to be 75° to limit the difference between these two cases to less than 10%.

To validate the efficacy of the plasmonic NSOM, we performed a nearfield scanning lithography experiment (Figure 4). In comparison with imaging applications, scan-

ning lithography can directly tell the local field confinement and also enhancement near the apexes of plasmonic NSOM probes. An AFM scanner (Bioscope, Digital Instrument) was used to scan our modified NSOM tip in close proximity to the sample surface. During the lithography, a laser beam at the wavelength of 365 nm (Spectra Physics) was coupled into the NSOM tip to expose the positive photoresist (IX965G, JSR Microelectronics Inc.) on a Si substrate (Figure 4a). By scanning the plasmonic NSOM probe on the top surface of the photoresist with an input laser power of 0.008 mW, a recorded pattern with a line width of 124 nm has been observed (Figure 4b). Without the plasmonic lens, the photoresist can never be exposed with such low input power (Figure 4c). Keeping the same scanning speed, a similar exposure result was obtained by using 10× higher input power (0.08 mW) through the tip without the plasmonic lens (Figure 4d). By comparing the depth and width of the fabricated patterns, doses from plasmonic NSOM probes are 2 × larger than those from normal NSOM probes. Considering that input power used is one order less for plasmonic NSOM probes, the local intensity of plasmonic NSOM probes should be ~20 times higher than that of normal NSOM probes. This result confirms the high resolution and high optical throughput of the plasmonic lenses.

The central concern of the conic plasmonic lens is how much energy can be concentrated into a focus point and how small the focus size is. Those aspects are strongly correlated and essentially are determined by parameters such as center aperture size, incident light frequency, and the metal and surrounding dielectrics. Smaller center aperture size gives better nearfield confinement but reduces enhancement, due to the lower contribution from the SPPs generated on the upper side of the plasmonic lens. The higher incident light frequency excites SPPs with shorter wavelength and thus provides smaller focus size, however, with reduced local intensity due to higher metal loss during the propagation. If the intensity is a more important concern, a longer wavelength should be used because the long SPP propagation length can support a larger plasmonic lens that focuses more energy to the center. The enhancement of plasmonic NSOM probes will be reduced when working in air condition, because the refraction index of the optical fiber on which plasmonic lenses are fabricated is higher (usually 1.47–1.52) than air and then SPPs cannot be generated on the air side of the lens. As we have mentioned before, this problem can be solved by applying microscope immersion oil to match the index. It has been shown that SPPs excited on a tapered plasmonic waveguide can introduce an adiabatic nanofocusing effect without subwavelength apertures,<sup>39,40</sup> but in our work, a center aperture on the plasmonic NSOM probe is still beneficial because it limits the focus size and increases the enhancement by constructive interference of SPPs on both sides of the metal coating. We must also point out that light propagating inside the fiber of plasmonic NSOM probes is actually not a plane wave. For more accurate estimation of local field enhancement, waveguide modes should be considered in calculations.

In this paper, we reported the development of an efficient plasmonic NSOM probe. The conic plasmonic lens, which consists of a 100 nm aperture surrounded by a circular grating, acts as a lens for focusing SPP waves at the NSOM probe. By utilizing circular grating to excite SPPs, tight focus of approximately a 100 nm spot was obtained at the center of the circular grating. Simulation results show that the light intensity at the focal point is enhanced 36× with respect to the intensity through a single aperture due to constructive interference of SPPs. A practical plasmonic NSOM system has been demonstrated experimentally for nearfield lithography for the first time. More than one order of enhancement of the local intensity has been observed in the experiment. The results indicate the potential of this scheme for use in nearfield nanolithography, high-density data storage, nano-spectroscopy, and high speed nanosensing applications.

**Acknowledgment.** This work was supported by the Air Force Office of Scientific Research Multidisciplinary University Research Initiative Program (grant no. FA9550-04-1-0434) and NSF NSEC under award no. DMI-0327077 and award no. 0404458.

## References

- (1) Dunn, R. C. *Chem. Rev.* **1999**, *99* (10), 2891–2927.
- (2) Brehm, M.; Taubner, T.; Hillenbrand, R.; Keilmann, F. *Nano Lett.* **2006**, *6* (7), 1307–1310.
- (3) Hsu, J. W. P. *Mater. Sci. Eng., R.* **2001**, *33* (1), 1–50.
- (4) Yu, N.; Diehl, L.; Cubukcu, E.; Pflugl, C.; David, B.; Scott, C.; Zhu, J.; Hofer, G.; Crozier, K. B.; Capasso, F. *Opt. Express* **2007**, *15* (20), 13227–13235.
- (5) Betzig, E.; Trautman, J. K.; Wolfe, R.; Gyorgy, E. M.; Finn, P. L.; Kryder, M. H.; Chang, C. H. *Appl. Phys. Lett.* **1992**, *61* (2), 142–144.
- (6) Valaskovic, G. A.; Holton, M.; Morrison, G. H. *Appl. Opt.* **1995**, *34* (7), 1215–1228.
- (7) Jin, E. X.; Xu, X. F. *Jpn. J. Appl. Phys., Part 1* **2004**, *43* (1), 407–417.
- (8) Matteo, J. A.; Fromm, D. P.; Yuen, Y.; Schuck, P. J.; Moerner, W. E.; Hesselink, L. *Appl. Phys. Lett.* **2004**, *85* (4), 648–650.
- (9) Sendur, K.; Challener, W. J. *Microsc. (Oxford)* **2003**, *210*, 279–283.
- (10) Sundaramurthy, A.; Schuck, P. J.; Conley, N. R.; Fromm, D. P.; Kino, G. S.; Moerner, W. E. *Nano Lett.* **2006**, *6* (3), 355–360.
- (11) Wang, L.; Uppuluri, S. M.; Jin, E. X.; Xu, X. F. *Nano Lett.* **2006**, *6* (3), 361–364.
- (12) Liu, Z. W.; Steele, J. M.; Sritravanich, W.; Pikus, Y.; Sun, C.; Zhang, X. *Nano Lett.* **2005**, *5* (9), 1726–1729.
- (13) Kim, D. W.; Kim, Y. C.; Suwal, O.; Jha, V.; Park, M. J.; Choi, S. S. *Mater. Sci. Eng., B* **2008**, *149* (3), 242–246.
- (14) Raether, H., *Surface plasmons on smooth and rough surfaces and on gratings*. Springer-Verlag: Berlin, 1988.
- (15) Smolyaninov, I. I. *J. Opt. A: Pure Appl. Opt.* **2005**, *7* (2), S165–S175.
- (16) Park, D. J.; Choi, S. B.; Ahn, K. J.; Kim, D. S.; Kang, J. H.; Park, Q. H.; Jeong, M. S.; Ko, D. K. *Phys. Rev. B* **2008**, *77* (11), 115451.
- (17) Sritravanich, W.; Fang, N.; Sun, C.; Luo, Q.; Zhang, X. *Nano Lett.* **2004**, *4* (6), 1085–1088.
- (18) Luo, X. G.; Ishihara, T. *Appl. Phys. Lett.* **2004**, *84* (23), 4780–4782.
- (19) Liu, Z. W.; Wei, Q. H.; Zhang, X. *Nano Lett.* **2005**, *5* (5), 957–961.
- (20) Heltzel, A.; Theppakuttai, S.; Chen, S. C.; Howell, J. R. *Nanotechnology* **2008**, *19* (2), 025305.
- (21) Tanaka, K.; Ohkubo, T.; Oumi, M.; Mitsuoka, Y.; Nakajima, K.; Hosaka, H.; Itao, K. *Jpn. J. Appl. Phys., Part 1* **2001**, *40* (3B), 1542–1547.
- (22) Wei, Q. H.; Su, K. H.; Durant, S.; Zhang, X. *Nano Lett.* **2004**, *4* (6), 1067–1071.
- (23) Tam, F.; Goodrich, G. P.; Johnson, B. R.; Halas, N. J. *Nano Lett.* **2007**, *7* (2), 496–501.
- (24) Ebbesen, T. W.; Lezec, H. J.; Ghaemi, H. F.; Thio, T.; Wolff, P. A. *Nature* **1998**, *391* (6668), 667–669.
- (25) Thio, T.; Ghaemi, H. F.; Lezec, H. J.; Wolff, P. A.; Ebbesen, T. W. *J. Opt. Soc. Am. B* **1999**, *16* (10), 1743–1748.

- (26) Krishnan, A.; Thio, T.; Kima, T. J.; Lezec, H. J.; Ebbesen, T. W.; Wolff, P. A.; Pendry, J.; Martin-Moreno, L.; Garcia-Vidal, F. J. *Opt. Commun.* **2001**, *200* (1–6), 1–7.
- (27) Lindquist, N. C.; Lesuffleur, A.; Oh, S. H. *Appl. Phys. Lett.* **2007**, *91* (25), 253105.
- (28) Park, T. H.; Mirin, N.; Lassiter, J. B.; Nehl, C. L.; Halas, N. J.; Nordlander, P. *ACS Nano* **2008**, *2* (1), 25–32.
- (29) Thio, T.; Pellerin, K. M.; Linke, R. A.; Lezec, H. J.; Ebbesen, T. W. *Opt. Lett.* **2001**, *26* (24), 1972–1974.
- (30) Lezec, H. J.; Degiron, A.; Devaux, E.; Linke, R. A.; Martin-Moreno, L.; Garcia-Vidal, F. J.; Ebbesen, T. W. *Science* **2002**, *297* (5582), 820–822.
- (31) Yin, L. L.; Vlasko-Vlasov, V. K.; Pearson, J.; Hiller, J. M.; Hua, J.; Welp, U.; Brown, D. E.; Kimball, C. W. *Nano Lett.* **2005**, *5* (7), 1399–1402.
- (32) Steele, J. M.; Liu, Z. W.; Wang, Y.; Zhang, X. *Opt. Express* **2006**, *14* (12), 5664–5670.
- (33) Lopez-Tejiera, F.; Rodrigo, S. G.; Martin-Moreno, L.; Garcia-Vidal, F. J.; Devaux, E.; Ebbesen, T. W.; Krenn, J. R.; Radko, I. P.; Bozhevolnyi, S. I.; Gonzalez, M. U.; Weeber, J. C.; Dereux, A. *Nat. Phys.* **2007**, *3* (5), 324–328.
- (34) Verhagen, E.; Kuipers, L.; Polman, A. *Nano Lett.* **2007**, *7* (2), 334–337.
- (35) Radko, I. P.; Bozhevolnyi, S. I.; Evlyukhin, A. B.; Boltasseva, A. *Opt. Express* **2007**, *15* (11), 6576–6582.
- (36) Feng, L.; Tetz, K. A.; Slutsky, B.; Lomakin, V.; Fainman, Y. *Appl. Phys. Lett.* **2007**, *91* (8), 081101–3.
- (37) Lide, D. R. *CRC Handbook of Chemistry and Physics*, electronic ed.; CRC Press: Boca Raton, FL, 2001.
- (38) Antosiewicz, T. J.; Szoplik, T. *Opt. Express* **2007**, *15* (17), 10920–10928.
- (39) Stockman, M. I. *Phys. Rev. Lett.* **2004**, *93* (13), 137404.
- (40) Ropers, C.; Neacsu, C. C.; Elsaesser, T.; Albrecht, M.; Raschke, M. B.; Lienau, C. *Nano Lett.* **2007**, *7* (9), 2784–2788.

NL8023824